The Astrophysical Journal Letters, 958:L25 (9pp), 2023 December 1 https://doi.org/10.3847/2041-8213/ad09d9

The Magnesium Isotope Composition of Samples Returned from Asteroid Ryugu

Martin Bizzarro[1,2], Martin Schiller[1], Tetsuya Yokoyama[3], Yoshinari Abe[4], Jérôme Aléon[5], Conel M. O'D. Alexander[6], Sachiko Amari[7,8], Yuri Amelin[9], Ken-ichi Bajo[10], Audrey Bouvier[11], Richard W. Carlson[12], Marc Chaussidon[2], Byeon-Gak Choi[12], Nicolas Dauphas[13], Andrew M. Davis[13], Tommaso Di Rocco[14], Wataru Fujiya[15], Ryota Fukai[16], Ikshu Gautam[3], Makiko K. Haba[3], Yuki Hibiya[17], Hiroshi Hidaka[18], Hisashi Homma[19], Peter Hoppe[20], Gary R. Huss[21], Kiyohiro Ichida[22], Tsuyoshi Iizuka[23], Trevor R. Ireland[24], Akira Ishikawa[3], Shoichi Itoh[25], Noriyuki Kawasaki[10], Noriko T. Kita[26], Kouki Kitajima[26], Thorsten Kleine[27], Shintaro Komatani[22], Alexander N. Krot[21], Ming-Chang Liu[28], Yuki Masuda[3], Mayu Morita[22], Fréderic Moynier[2], Kazuko Motomura[29], Izumi Nakai[30], Kazuhide Nagashima[21], David Nesvorný[30], Ann Nguyen[31], Larry Nittler[5], Morihiko Onose[22], Andreas Pack[14], Changkun Park[32], Laurette Piani[33], Liping Qin[34], Sara S. Russell[35], Naoya Sakamoto[36], Maria Schönbächler[37], Lauren Tafla[29], Haolan Tang[29], Kentaro Terada[38], Yasuko Terada[39], Tomohiro Usui[16], Sohei Wada[10], Meenakshi Wadhwa[40], Richard J. Walker[41], Katsuyuki Yamashita[42], Qing-Zhu Yin[43], Shigekazu Yoneda[44], Edward D. Young[29], Hiroharu Yui[45], Ai-Cheng Zhang[46], Tomoki Nakamura[47], Hiroshi Naraoka[48], Takaaki Noguchi[25], Ryuji Okazaki[48], Kanako Sakamoto[16], Hikaru Yabuta[49], Masanao Abe[16], Akiko Miyazaki[16], Aiko Nakato[16], Masahiro Nishimura[16], Tatsuaki Okada[16], Toru Yada[16], Kasumi Yogata[16], Satoru Nakazawa[16], Takanao Saiki[16], Satoshi Tanaka[16], Fuyuto Terui[50], Yuichi Tsuda[16], Sei-ichiro Watanabe[18], Makoto Yoshikawa[16], Shogo Tachibana[51], and Hisayoshi Yurimoto[10]

[1] Centre for Star and Planet Formation, Globe Institute, University of Copenhagen, DK-1350 Copenhagen K, Denmark; bizzarro@sund.ku.dk
[2] Université Paris Cité, Institut de Physique du Globe de Paris, CNRS, F-75005 Paris, France
[3] Department of Earth and Planetary Sciences, Tokyo Institute of Technology, Tokyo 152-8551, Japan
[4] Graduate School of Engineering Materials Science and Engineering, Tokyo Denki University, Tokyo 120-8551, Japan
[5] Institut de Minéralogie, de Physique des Matériaux et de Cosmochimie, Sorbonne Université, Museum National d'Histoire Naturelle, CNRS UMR 7590, IRD, F-75005 Paris, France
[6] Earth and Planets Laboratory, Carnegie Institution for Science, Washington, DC 20015, USA
[7] McDonnell Center for the Space Sciences and Physics Department, Washington University, St. Louis, MO 63130, USA
[8] Geochemical Research Center, The University of Tokyo, Tokyo 113-0033, Japan
[9] Korea Basic Science Institute, Ochang, Cheongwon, Cheongju, Chungbuk 28119, Republic of Korea
[10] Natural History Sciences, IIL, Hokkaido University, Sapporo 001-0021, Japan
[11] Bayerisches Geoinstitut, Universität Bayreuth, D-95447 Bayreuth, Germany
[12] Department of Earth Science Education, Seoul National University, Seoul 08826, Republic of Korea
[13] Department of the Geophysical Sciences and Enrico Fermi Institute, The University of Chicago, 5734 South Ellis Avenue, Chicago, IL 60637, USA
[14] Faculty of Geosciences and Geography, University of Göttingen, D-37077 Göttingen, Germany
[15] Faculty of Science, Ibaraki University, Mito 310-8512, Japan
[16] ISAS/JSEC, JAXA, Sagamihara 252-5210, Japan
[17] General Systems Studies, The University of Tokyo, Tokyo 153-0041, Japan
[18] Earth and Planetary Sciences, Nagoya University, Nagoya 464-8601, Japan
[19] Osaka Application Laboratory, SBUWDX, Rigaku Corporation, Osaka 569-1146, Japan
[20] Max Planck Institute for Chemistry, D-55128 Mainz, Germany
[21] Hawai'i Institute of Geophysics and Planetology, University of Hawai'i at Mānoa; Honolulu, HI 96822, USA
[22] Analytical Technology, Horiba Techno Service Co., Ltd., Kyoto 601-8125, Japan
[23] Earth and Planetary Science, The University of Tokyo, Tokyo 113-0033, Japan
[24] School of Earth and Environmental Sciences, The University of Queensland, St Lucia, QLD 4072, Australia
[25] Earth and Planetary Sciences, Kyoto University, Kyoto 606-8502, Japan
[26] Geoscience, University of Wisconsin-Madison, Madison, WI 53706, USA
[27] Max Planck Institute for Solar System Research, D-37077 Göttingen, Germany
[28] Earth, Planetary, and Space Sciences, UCLA, Los Angeles, CA 90095, USA
[29] Thermal Analysis, Rigaku Corporation, Tokyo 196-8666, Japan
[30] Department of Space Studies, Southwest Research Institute, Boulder, CO 80302, USA
[31] Astromaterials Research and Exploration Science, NASA Johnson Space Center, Houston, TX 77058, USA
[32] Earth-System Sciences, Korea Polar Research Institute, Incheon 21990, Republic of Korea
[33] Centre de Recherches Pétrographiques et Géochimiques, CNRS—Université de Lorraine, F-54500 Nancy, France
[34] University of Science and Technology of China, School of Earth and Space Sciences, Anhui 230026, People's Republic of China
[35] Department of Earth Sciences, Natural History Museum, London SW7 5BD, UK
[36] IIL, Hokkaido University, Sapporo 001-0021, Japan
[37] Institute for Geochemistry and Petrology, Department of Earth Sciences, ETH Zurich, Zurich, Switzerland
[38] Earth and Space Science, Osaka University, Osaka 560-0043, Japan
[39] Spectroscopy and Imaging, Japan Synchrotron Radiation Research Institute, Hyogo 679-5198 Japan
[40] School of Earth and Space Exploration, Arizona State University, Tempe, AZ 85281, USA
[41] Geology, University of Maryland, College Park, MD 20742, USA
[42] Graduate School of Natural Science and Technology, Okayama University, Okayama 700-8530, Japan
[43] Earth and Planetary Sciences, University of California, Davis, CA 95616, USA
[44] Science and Engineering, National Museum of Nature and Science, Tsukuba 305-0005, Japan
[45] Chemistry, Tokyo University of Science, Tokyo 162-8601, Japan
[46] School of Earth Sciences and Engineering, Nanjing University, Nanjing 210023, People's Republic of China
[47] Department of Earth Science, Tohoku University, Sendai 980-8578, Japan
[48] Department of Earth and Planetary Sciences, Kyushu University, Fukuoka 819-0395, Japan
[49] Earth and Planetary Systems Science Program, Hiroshima University, Higashi-Hiroshima 739-8526, Japan

[50] Kanagawa Institute of Technology, Atsugi 243-0292, Japan
[51] UTokyo Organization for Planetary and Space Science, University of Tokyo, Tokyo 113-0033, Japan
Received 2023 September 16; revised 2023 October 25; accepted 2023 November 3; published 2023 November 24

Abstract

The nucleosynthetic isotope composition of planetary materials provides a record of the heterogeneous distribution of stardust within the early solar system. In 2020 December, the Japan Aerospace Exploration Agency Hayabusa2 spacecraft returned to Earth the first samples of a primitive asteroid, namely, the Cb-type asteroid Ryugu. This provides a unique opportunity to explore the kinship between primitive asteroids and carbonaceous chondrites. We report high-precision $\mu^{26}Mg^{*}$ and $\mu^{25}Mg$ values of Ryugu samples together with those of CI, CM, CV, and ungrouped carbonaceous chondrites. The stable Mg isotope composition of Ryugu aliquots defines $\mu^{25}Mg$ values ranging from -160 ± 20 ppm to -272 ± 30 ppm, which extends to lighter compositions relative to Ivuna-type (CI) and other carbonaceous chondrite groups. We interpret the $\mu^{25}Mg$ variability as reflecting heterogeneous sampling of a carbonate phase hosting isotopically light Mg ($\mu^{25}Mg \sim -1400$ ppm) formed by low temperature equilibrium processes. After correcting for this effect, Ryugu samples return homogeneous $\mu^{26}Mg^{*}$ values corresponding to a weighted mean of 7.1 ± 0.8 ppm. Thus, Ryugu defines a $\mu^{26}Mg^{*}$ excess relative to the CI and CR chondrite reservoirs corresponding to 3.8 ± 1.1 and 11.9 ± 0.8 ppm, respectively. These variations cannot be accounted for by in situ decay of ^{26}Al given their respective $^{27}Al/^{24}Mg$ ratios. Instead, it requires that Ryugu and the CI and CR parent bodies formed from material with a different initial $^{26}Al/^{27}Al$ ratio or that they are sourced from material with distinct Mg isotope compositions. Thus, our new Mg isotope data challenge the notion that Ryugu and CI chondrites share a common nucleosynthetic heritage.

Unified Astronomy Thesaurus concepts: Solar system evolution (2293); Asteroids (72); Carbonaceous chondrites (200); Meteorite composition (1037); Nucleosynthesis (1131)

1. Introduction

The solar system's rocky planets and asteroidal bodies record nucleosynthetic isotope variability for several elements, which is interpreted to reflect the heterogeneous distribution of stardust from different stellar sources in the protoplanetary disk (Dauphas & Schauble 2016). A key cosmochemical observation is the existence of a gradient in the nucleosynthetic composition of planetary materials with orbital distance. For example, inner solar system bodies typically record depletion in the abundance of iron-group element neutron-rich isotopes relative to the terrestrial composition (i.e., ^{54}Cr, ^{50}Ti, and ^{48}Ca), whereas bodies inferred to have accreted beyond Jupiter are characterized by excesses in these isotopes (Trinquier et al. 2007, 2009; Schiller et al. 2015). Although the origin of the solar system's nucleosynthetic variability is debated, it can be used to infer genetic relationships between early formed bodies and, ultimately, provide constraints on their accretion regions.

In 2020 December, the Japan Aerospace Exploration Agency Hayabusa2 spacecraft returned to Earth the first samples of a primitive asteroid, namely, the Cb-type asteroid Ryugu (162173; Watanabe et al. 2019; Tachibana et al. 2022). This provides a unique opportunity to explore the kinship between primitive asteroids and various types of carbonaceous chondrites recovered on Earth. Based on chemistry, mineralogy, petrology, and isotope systematics of various elements, it has been proposed that Ryugu samples are closely related to Ivuna-type (CI) carbonaceous chondrites (Yokoyama et al. 2023a). Indeed, their bulk ^{54}Cr and ^{50}Ti isotopic signatures and the chemical abundances of most elements are within the range of CI chondrites. Moreover, like CIs, Ryugu samples experienced extensive aqueous alteration in the presence of water and mainly consist of hydrous silicates (serpentine and saponite) and other secondary minerals (i.e., carbonate, magnetite, and sulfide) interpreted to have formed during asteroidal fluid circulation (Ito et al. 2022; Nakamura et al. 2022; Nakamura et al. 2023; Yamaguchi et al. 2023; Yokoyama et al. 2023a).

It has been suggested that Ryugu and CI chondrites may have accreted in a disk region distinct from most parent bodies of carbonaceous chondrites, possibly in the same formation region as cometary bodies (Hopp et al. 2022; Kawasaki et al. 2022). In this model, the parent bodies of most carbonaceous chondrites are hypothesized to have accreted within the orbits of Jupiter and Saturn, whereas Ryugu and CI chondrites accreted in an isotopically distinct reservoir located further out in the disk, perhaps in the vicinity of the formation region of Uranus and Neptune. This implies that Ryugu and CI chondrites may share a common nucleosynthetic heritage with Oort cloud comets. If correct, the nucleosynthetic fingerprint of Ryugu and CI chondrites can be used as proxy for that of cometary material, which is central to understanding the origin of the solar system's nucleosynthetic variability as well as early disk dynamics.

High-precision Mg isotope (^{24}Mg, ^{25}Mg, and ^{26}Mg) measurements can provide a novel perspective on the kinship between Ryugu with CI chondrites and, by extension, the accretion region of Cb-type asteroids. Magnesium isotope variability in solar system materials can originate from the decay of the short-lived ^{26}Al nuclide (Lee et al. 1976) as well as primary nucleosynthetic processes (Wasserburg et al .2012; Park et al. 2017; Larsen et al. 2020), similarly to that recorded by tracers such as ^{54}Cr, ^{50}Ti, and ^{48}Ca. Moreover, Mg isotopes can also be fractionated according to their masses by high-temperature events in the protoplanetary disk or, alternatively, by low-temperature parent-body secondary processes (Young & Galy 2004). Thus, the combination of high-precision mass-independent and mass-dependent Mg isotope compositions is useful to understand genetic relationships and accretion history of planetary materials. In this Letter, we report the isotopic composition of Mg as well as the Al/Mg ratios of Ryugu samples from the first and second touchdown sites. These measurements are complemented by additional analyses of the

Mg isotope composition of several CM (Mighei-type), CV (Vigarano-type), and ungrouped carbonaceous chondrites, including six individual small aliquots of the Orgueil CI chondrites to document the extend of isotopic heterogeneity in individual CIs.

2. Material and Methods

The samples investigated in this study include two Ryugu samples from the first touchdown site (A0106, A0106-A0107), two Ryugu samples from the second touchdown site (C0107, C0108), Tarda and Tagish Lake (C ungrouped), Murchison (CM), and Allende (CV). The masses of the Ryugu A0106, A0106-A0107, C0107, and C0108 samples processed were 14.61, 23.88, 12.78, and 22.24 mg, respectively, whereas approximately 25–30 mg of the various chondrites was processed. Sample digestion and chemical purification for these samples was conducted as described in Yokoyama et al. (2023a). Elemental abundances were determined on chemically unpurified aliquots of the samples (Yokoyama et al. 2023a). We also investigated six 25–30 mg aliquots of the Orgueil CI chondrite, which were digested using HF-HNO_3 mixtures in Parr Bombs at the Centre for Star and Planet Formation (University of Copenhagen).

The Ryugu, Tarda, Tagish Lake, Murchison, and Allende samples were prepurified Na–K–Mg–Ni cuts derived from the chemical separation described in Yokoyama et al. (2023a) containing around 100 μg of Mg. For Mg purification, samples were dried down, converted to nitric form and taken up in 150 μL of 10 mmol HNO_3. Sample solutions were processed using a ThermoFisher Scientific Dionex ICS-6000 system with attached fraction collector. Samples were injected onto a 250 ×5 mm CS16 column, and subsequently Mg was separated from the remaining matrix elements via elution of increasing molarity of HCl at a constant flow rate of 1 mL minute^{-1}. In detail, the elution proceeded in 20 mL steps of 7.5 mmol, 15 mmol, 22.5 mmol, and 30 mmol. Mg was collected in a 7 mL elution volume from 55 mL to 62 mL. After sample elution, the column was cleaned via elution of 1 M HCl + 75 mmol HF and reconditioned for the next sample. After Mg purification, samples were dried down, converted to nitric acid, and taken up in 2.5% HNO_3 for isotope analysis. Magnesium was chemically purified for the six 25–30 mg aliquots of the Orgueil CI chondrite according to protocols described in Bizzarro et al. (2011).

Magnesium isotope measurements were conducted using a ThermoScientific Neptune multicollector inductively coupled plasma mass spectrometer housed at the Centre for Star and Planet Formation (University of Copenhagen). The analytical approach followed established procedures at this laboratory (Bizzarro et al. 2011; Larsen et al. 2016; Olsen et al. 2016). In short, samples were introduced to the instrument using an ESI Apex Q desolvator with an attached membrane desolvation unit at typical aspiration rates of 50 μl minute^{-1}. Measurements of the ^{24}Mg, ^{25}Mg, and ^{26}Mg isotopes were performed in medium-resolution mode. Sample measurements were bracketed by measurements of Mg purified from the rock standard DTS-2b that was used to correct for instrumental mass fractionation. Each analysis consisted of 100 cycles with an integration time of 16.77 s. The sensitivity for ^{24}Mg was ∼40 V per ppm and measurements were conducted at total beam signals of ∼50 V. The raw data were reduced using the software Iolite4. The mass-dependent ^{25}Mg/^{24}Mg ratio was calculated and expressed as μ^{25}Mg values in ppm relative to the DSM-3 standard as follows: $\mu^{25}\mathrm{Mg} = [(^{25}\mathrm{Mg}/^{24}\mathrm{Mg})_{\mathrm{sample}}/(^{25}\mathrm{Mg}/^{24}\mathrm{Mg})_{\mathrm{standard}} - 1] \times 10^6$. The mass-independent ^{26}Mg/^{24}Mg ratio (μ^{26}Mg*) is reported in the same fashion and calculated by internal normalization to ^{25}Mg/^{24}Mg = 0.126896 (Bizzarro et al. 2011) on an individual ratio basis using the exponential mass fractionation law. The ^{27}Al/^{24}Mg ratios for sample A0106 and A0108 were determined using the ThermoScientific quadrupole ICP-MS iCAP at the Centre for Star and Planet Formation (University of Copenhagen) using 0.5% aliquots of the original sample dissolution.

3. Results

The Mg isotope compositions and ^{27}Al/^{24}Mg ratios of samples analyzed here are reported in Table 1. The six small aliquots of Orgueil return μ^{26}Mg* values ranging from -0.8 ± 1.4 to 2.8 ± 1.5 ppm, defining a weighted mean of 1.5 ± 1.0 ppm. This value is within analytical uncertainty of four high-precision estimates for Orgueil of 4.3 ± 2.2 and 2.1 ± 2.8 reported by Larsen et al. (2011) and Luu et al. (2019), respectively. Similarly, the μ^{26}Mg* of 8.9 ± 2.8 ppm obtained for Murchison is within analytical uncertainty of previously published values (Luu et al. 2019; van Kooten et al. 2020). Although no literature data exist for Tagish Lake and Tarda, our measurements for these two anomalous carbonaceous chondrites fall within the range of μ^{26}Mg* values previously reported for CM chondrites (van Kooten et al. 2016; Luu et al. 2019; van Kooten et al. 2020). The Allende chondrite contains abundant refractory inclusions such that its Mg isotope composition can vary due to heterogeneous sampling of this material, especially for small sample sizes. However, the μ^{26}Mg*value and ^{27}Al/^{24}Mg ratio defined here compare favorably with earlier estimates reported by Larsen et al. (2016) and Luu et al. (2019).

The four Ryugu samples define μ^{26}Mg* values ranging from 7.2 ± 1.2 to 10.9 ± 1.7 ppm, which are distinct from the μ^{26}Mg* values of the three CI chondrites Alais, Orgueil, and Ivuna of 3.7 ± 1.5, 2.0 ± 0.9, and 4.1 ± 0.8, respectively (Larsen et al. 2011; Luu et al. 2019). The elevated μ^{26}Mg* values recorded by Ryugu samples could, in principle, be explained by radiogenic ingrowth from the short-lived ^{26}Al nuclide, requiring that Ryugu is characterized by a super solar ^{27}Al/^{24}Mg value. However, the ^{27}Al/^{24}Mg ratios measured for the four Ryugu samples return values ranging from 0.0901 to 0.0972 (Table 1), which are marginally lower than the solar value of 0.09781 ± 0.00029 defined from a 2.8 g aliquot of the Ivuna CI chondrite (Paton et al. 2012). The sample with least anomalous μ^{26}Mg* of 7.2 ± 1.2 ppm is characterized by the highest ^{27}Al/^{24}Mg ratios of the four Ryugu aliquots, establishing the observed μ^{26}Mg* cannot be accounted for by in situ decay of ^{26}Al that should result in the largest μ^{26}Mg* value. We note that ^{27}Al/^{24}Mg ratios have been previously determined for 18 Ryugu particles, which range from 0.081 to 0.102 (Nakamura et al. 2022). Including the ^{27}Al/^{24}Mg ratios determined here for A0106, A0106-A0107, C0107, and C0108, we calculate a weighted mean of 0.09487 ± 0.00062 (excluding two outliers), which we consider as the best estimate of the ^{27}Al/^{24}Mg ratio of Ryugu. This estimate is approximately 3% lower than the solar value. Thus, a key observation of this work is that Ryugu is characterized by an anomalous Mg isotope composition relative to CI chondrites and other carbonaceous chondrites with near solar ^{27}Al/^{24}Mg ratios (Figure 1(a)).

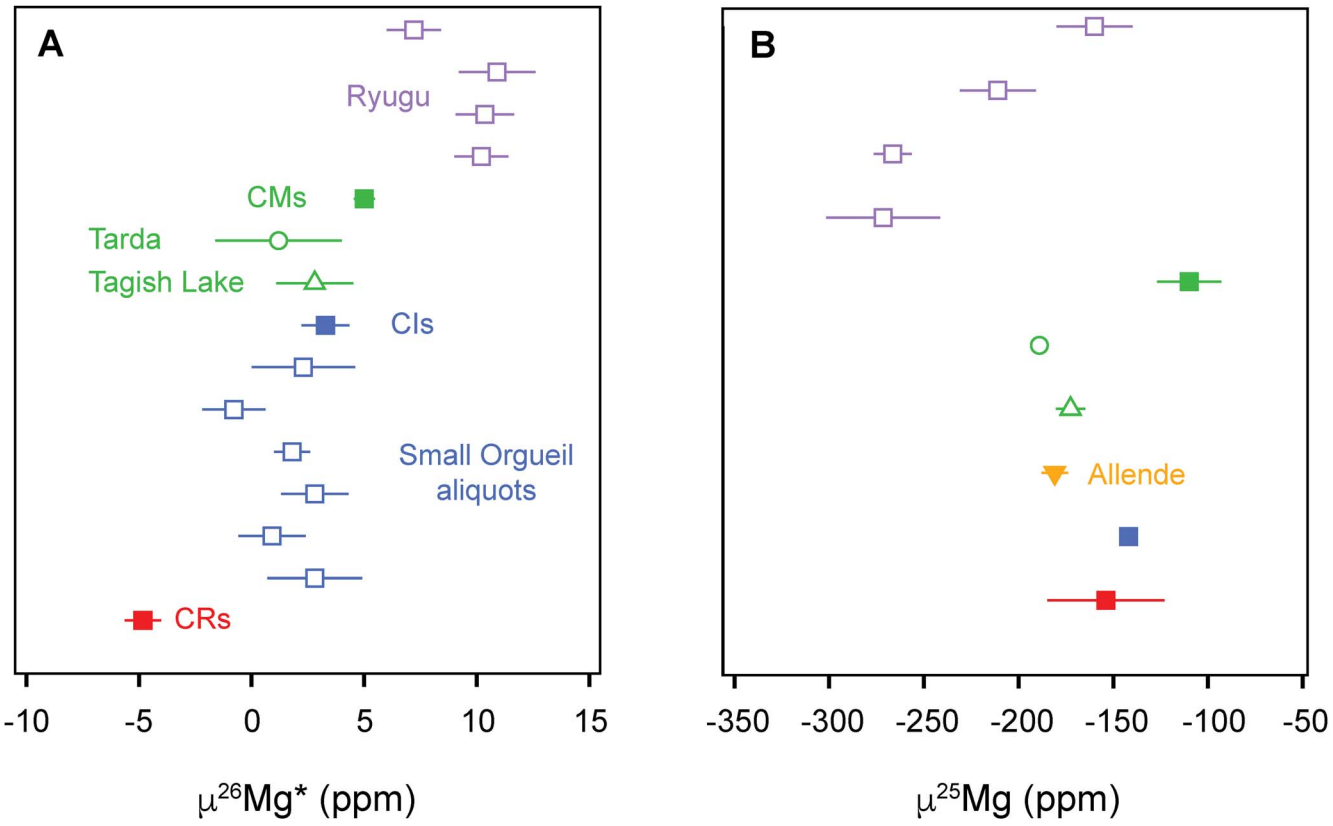

Figure 1. The $\mu^{26}Mg^{*}$ (A) and $\mu^{25}Mg$ (B) values of Ryugu samples and carbonaceous chondrites analyzed here. Solid symbols reflect the weighted means of several meteorite samples, whereas open symbols are individual meteorites. The weighted means include data from Larsen et al. (2011, 2016), van Kooten et al. (2016), Luu et al. (2019), and van Kooten et al. (2020). Error bars represent the internal precision (2SE) for individual samples and 95% confidence intervals for weighted means.

Table 1
The Mg Isotope Composition, Al/Mg Ratios, as well as the Ca Abundance and Ca/Mg Ratios of Ryugu Samples and Carbonaceous Chondrites Investigated in This Study

Sample	$^{27}Al/^{24}Mg$[a]	$^{27}Al/^{24}Mg$[b]	$\mu^{26}Mg^{*}$	$\mu^{26}Mg^{*}_{corr}$	$\mu^{25}Mg$	*N*	[Ca] wt.%[b]	Ca/Mg[b]
Ryugu								
A0106		0.090	9.6 ± 3.0		−286 ± 10	10	3.00 ± 0.07	0.266 ± 0.016
Repeat			10.8 ± 1.6		−257 ± 10	10		
Average + 2SE			*10.2 ± 1.2*	*6.0 ± 1.8*	*−272 ± 25*			
C0107		0.094	11.0 ± 4.2		−263 ± 17	10	2.47 ± 0.06	0.250 ± 0.016
Repeat			9.7 ± 2.0		−270 ± 11	10		
Average + 2SE			*10.4 ± 1.3*	*6.4 ± 1.5*	*−267 ± 10*			
A0106-A107	0.091	0.091	10.9 ± 1.7	9.0 ± 2.0	−212 ± 20	10	1.63 ± 0.08	0.153 ± 0.008
C0108	0.096	0.097	7.2 ± 1.2	7.2 ± 1.2	−162 ± 20	10	1.37 ± 0.09	0.132 ± 0.009
Chondrites								
Tarda	0.105	0.106	2.8 ± 1.7		−173 ± 8	10		
Tagish Lake	0.104	0.103	1.2+2.8		−190 ± 5	10		
Allende	0.130	0.130	16.3 ± 1.8		−217 ± 10	10		
Murchison	0.108	0.108	8.9 ± 2.8		−130 ± 24	10		
Orgueil-1			2.8 ± 2.1		−144 ± 13	10		
Orgueil-2			0.9 ± 1.5		−266 ± 14	10		
Orgueil-3			2.8 ± 1.5		−129 ± 10	10		
Orgueil-4			1.8 ± 0.8		−147 ± 15	10		
Orgueil-5			−0.8 ± 1.4		−147 ± 21	10		
Orgueil-6			2.3 ± 2.3		−137 ± 35	10		

Notes.
[a] Measured in Copenhagen by ICPMS.
[b] Measured at Tokyo Tech by ICPMS.

The stable Mg isotope composition of Ryugu aliquots define $\mu^{25}Mg$ values ranging from −160 ± 20 ppm to −272 ± 30 ppm relative to DSM-3, which extends to lighter compositions relative to CI and other carbonaceous chondrite groups (Figure 1(b)). We note that the lightest compositions are recorded by the samples C0107 and A0106, which are the

smallest aliquots with masses of 12.78 and 14.61 mg relative to A0106-A0107 and C0108 that have masses of 23.88 and 22.24 mg. Thus, a possibility is that the μ^{25}Mg variability observed in Ryugu is due to heterogeneous sampling of a phase characterized by a light Mg isotope composition relative to bulk CI chondrites.

4. Discussion

4.1. Origin of the Mg Isotope Variability Recorded by Ryugu Samples

Exposure to galactic cosmic rays or incomplete digestion of presolar grains could potentially induce variations in μ^{26}Mg* among Ryugu samples. However, Mg isotopes have small thermal neutron-capture cross sections (0.054–0.200 barn; Walkiewicz et al. 1992) and coupled with the short cosmic-ray exposure ages of 5 Myr for Ryugu samples (Okazaki et al. 2023) means that it is unlikely that the Mg isotope composition of Ryugu is affected by cosmogenic effects. Step-leaching experiments provide meaningful information to assess the role of incomplete digestion of refractory presolar grains to account for the anomalous μ^{26}Mg* values of Ryugu relative to CI chondrites. Schiller et al. (2015) reported high-precision Mg isotope data for a 2.8 g aliquot of the Ivuna CI chondrite. The μ^{26}Mg* values of individual step-leaches demonstrate that the Mg hosted in chemically resistant and likely refractory phases is characterized by highly positive μ^{26}Mg* values of up to 1604.3 ± 1.0 ppm. Thus, incomplete dissolution of refractory phases would result in lowering the μ^{26}Mg* values and, as such, cannot account for the elevated μ^{26}Mg* of Ryugu samples relative to CIs.

Given that the Ryugu samples record μ^{25}Mg variability, we explore whether inappropriate correction for natural mass-dependent fractionation could account for the anomalous μ^{26}Mg* values defined by Ryugu samples. During acquisition of high-precision Mg isotope measurements by MC-ICPMS, mass discrimination is corrected for by assuming that both instrumental and natural mass fractionation affecting the samples follow a kinetic mass fractionation law. Thus, if a component of the samples' natural mass fractionation is driven by equilibrium processes, it will result in apparent residual effects on the corrected μ^{26}Mg* values. In particular, light isotope fractionation by equilibrium processes results in apparent excesses in the μ^{26}Mg* values when correcting for mass discrimination correction with the kinetic law (Bizzarro et al. 2011). A potential host of isotopically light Mg in chondrites is secondary carbonate minerals that formed as a result of parent-body aqueous alteration, which in Ryugu is dominated by dolomite (Nakamura et al. 2022). Precipitation of dolomite during aqueous alteration on Ryugu has been inferred to have occurred at a temperature of 37 ± 10°C (Yokoyama et al. 2023a). At such temperatures, stable isotope fractionation of Mg during dolomite formation is driven by equilibrium processes and, in addition, ab initio calculation indicates that the Mg hosted in dolomite will be isotopically light by several per mille relative to the fluid (Schauble 2011).

Dolomite in Ryugu is inferred to be the main carrier phase of Ca such that the Ca abundance can be used as a proxy to estimate the relative amount of dolomite in individual samples (Moynier et al. 2022). Figures 2(a) and (b) show that the μ^{25}Mg values covary with both the Ca abundance and the Ca/Mg ratio in Ryugu samples, with CI chondrites defining a compositional endmember. This observation establishes that the observed range of μ^{25}Mg values results from variable incorporation of dolomite hosting isotopically light Mg. Based on the linear relationship defined by Ryugu samples and CI chondrites (Figures 2(a) and (b)), we use the Ca abundance and Ca/Mg ratio measured for Ryugu dolomite grains (Bazi et al. 2022) to iteratively determine the μ^{25}Mg composition of the dolomite endmember that minimizes the scatter as measured by the mean square of weighted deviations (M.S.W.D.). Because the μ^{25}Mg values are unrelated to the Ca abundance and the Mg abundance in dolomite is nearly identical to that of bulk Ryugu, a linear relationship is expected in both cases. Figures 2(c) and (d) show that a μ^{25}Mg value of -1400 ppm for the dolomite endmember results in statistically acceptable fits for both relationships. This μ^{25}Mg estimate is strikingly consistent with that inferred *by* ab initio calculations of the Mg isotope composition of dolomites precipitated at temperatures comparable to that deduced for the aqueous alteration on Ryugu (Schauble 2011; Yokoyama et al. 2023a). Using this endmember composition, mass balance calculations show that the μ^{25}Mg variability can be accounted for by assimilation of up to 10% dolomite, which is similar to Ryugu's most dolomite-rich particles (Nakamura et al. 2022). We note that a light μ^{25}Mg value of -1340 ± 20 ppm has been recently determined for breunnerite (Mg, Fe, Mn)CO_3 extracted from Ryugu particle C0002 (Yoshimura et al. 2023), in agreement with our results and interpretation.

Apart from sample C0108, which has a μ^{25}Mg value indistinguishable from bulk CI chondrites, the remaining Ryugu aliquots are interpreted to be affected by heterogeneous sampling of a phase containing light Mg fractionated by equilibrium processes. Theoretical considerations indicate that the apparent excess in the μ^{26}Mg* value resulting from inappropriate mass discrimination correction is at most 3.75 ppm per 100 ppm of mass-dependent fractionation as recorded by the μ^{25}Mg value, considering the offset between the equilibrium and kinetic mass fractionation laws (Bizzarro et al. 2011). Thus, we calculate the difference between the μ^{25}Mg value of C0108 and the remaining Ryugu samples to correct for this effect, accounting for the μ^{25}Mg uncertainties. After correction, the four Ryugu samples define a narrow range of μ^{26}Mg$^*_{corr}$ values from 6.0 ± 1.8 to 9.0 ± 2.0 ppm that are identical within uncertainty (μ^{26}Mg$^*_{corr}$; Table 1). Using a weighted mean approach, we calculate an average value of 7.1 ± 0.8 ppm, which we consider is the best estimate for the bulk μ^{26}Mg* value of Ryugu.

4.2. Excess ^{26}Mg* in Ryugu

Figure 3 shows our best estimate for the bulk μ^{26}Mg* value of Ryugu plotted together with the weighted means of CR (Renazzo-type) and CI chondrites. Ryugu defines a μ^{26}Mg* excess relative to the CI and CR chondrite reservoirs corresponding to 3.8 ± 1.1 and 11.9 ± 0.8 ppm, respectively. Albeit small, these variations are clearly resolved and cannot be accounted for by in situ decay of ^{26}Al assuming homogeneous distribution of this nuclide across solar system reservoirs given their respective bulk ^{27}Al/^{24}Mg ratios. Instead, it requires that Ryugu and the parent bodies of CI and CR chondrites formed from material with a different initial abundance of ^{26}Al or, alternatively, that they are sourced from material with distinct Mg isotope compositions.

Heterogeneous distribution of ^{26}Al in the early solar system can stem from variable incorporation of a stellar-derived, carrier phase of ^{26}Al or, alternatively, variable incorporation of circumsolar material irradiated by particles emitted by the

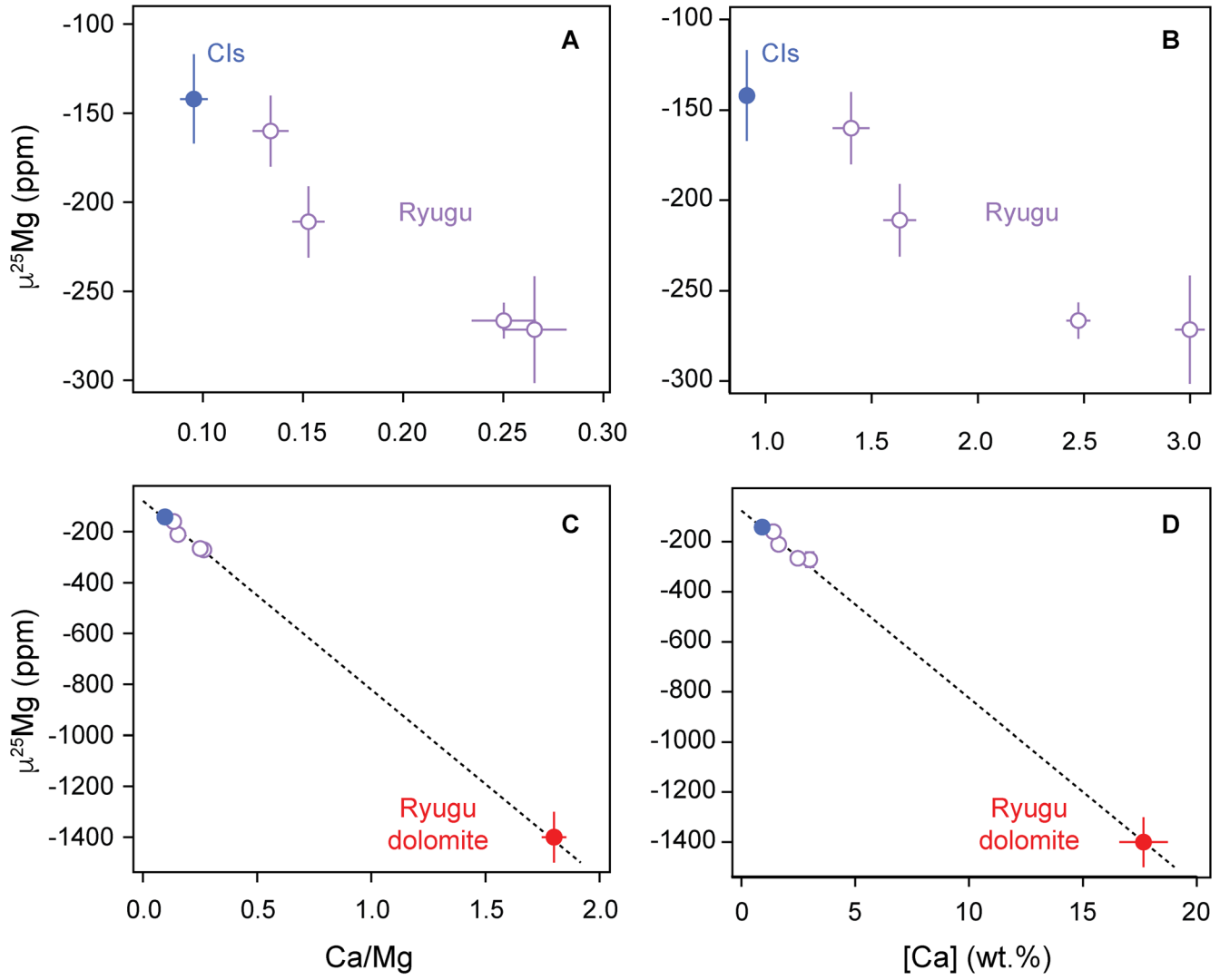

Figure 2. Variation diagrams showing the relationships between the μ^{25}Mg values of CI chondrites, Ryugu bulk samples, and inferred Ryugu dolomite and their Ca/Mg ratios and Ca abundance. The CI chondrite μ^{25}Mg value reflects the weighted mean of Orgueil, Ivuna, and Alais based on data from this study and Larsen et al. (2011) and Luu et al. (2019). The Ca abundance and Ca/Mg ratio for CI chondrites are from Palme et al. (2014). The Ca abundance and Ca/Mg ratio for the Ryugu dolomite are from Bazi et al. (2022). The μ^{25}Mg value of Ryugu dolomite was determined iteratively to minimize the scatter as measured by the M.S.W.D. Using a μ^{25}Mg of −1400 returns an M.S.W.D. of 1.6 and 2.6 for panels (C) and (D), respectively. Apart from CI chondrite, where we used a 95% confidence interval, all other uncertainties represent the internal precisions (2SE). For the Ryugu dolomite μ^{25}Mg value, we used an uncertainty estimate of 100 ppm.

energetic proto-Sun, which can result in the production of spallogenic ^{26}Al (Gounelle et al. 2001). Although the exact origin of a potential ^{26}Al heterogeneity does not impact the main observations or interpretations presented in our work, we note that two lines of evidence do not support the irradiation scenario. First, intense irradiation of solids is expected to result in measurable collateral effects in the spallation sensitive nuclide ^{150}Sm. However, the ^{150}Sm compositions determined for Ryugu and other carbonaceous chondrites do not covary with the μ^{26}Mg* values reported here (Carlson et al. 2007; Torrano et al. 2023). Second, solids formed and irradiated during an early, active phase of the proto-Sun are predicted to have an ^{16}O-rich, solar oxygen isotope composition akin to that recorded by calcium–aluminum-rich inclusions (Krot et al. 2010). Given that Ryugu records an excess in μ^{26}Mg* relative to other carbonaceous chondrites, its oxygen isotope composition should be the most ^{16}O-rich. Yet, the mass-independent oxygen isotope composition is the least ^{16}O-rich among the carbonaceous asteroids (Greenwood et al. 2023).

Because many chondrite groups are variably affected by radiogenic ingrowth from in situ decay of ^{26}Al given their observed range in bulk Al/Mg ratios, it is useful to correct for radiogenic ingrowth to facilitate comparison of their initial Mg isotope compositions with that of Ryugu. Figure 4 shows the μ^{26}Mg* values corrected for radiogenic ingrowth of Ryugu, CI and CR chondrites plotted together with that of CM, CO (Ornans-type) and CV, CK (Karonda-type) carbonaceous chondrites, as well as Tarda and Tagish Lake, assuming that all groups formed with an initial ^{26}Al/^{27}Al ratio of $\sim 5.2 \times 10^{-5}$ (Jacobsen et al. 2008; Larsen et al. 2011). After correcting for radiogenic ingrowth, the initial μ^{26}Mg* offsets between Ryugu and the CI and CR groups become 4.8 ± 1.3 and 13.3 ± 1.3, respectively. All carbonaceous chondrite groups record initial μ^{26}Mg* values that are intermediate between Ryugu and CR chondrites, establishing that Ryugu and CRs define compositional endmembers that can account for the initial μ^{26}Mg* variability recorded by carbonaceous chondrite groups.

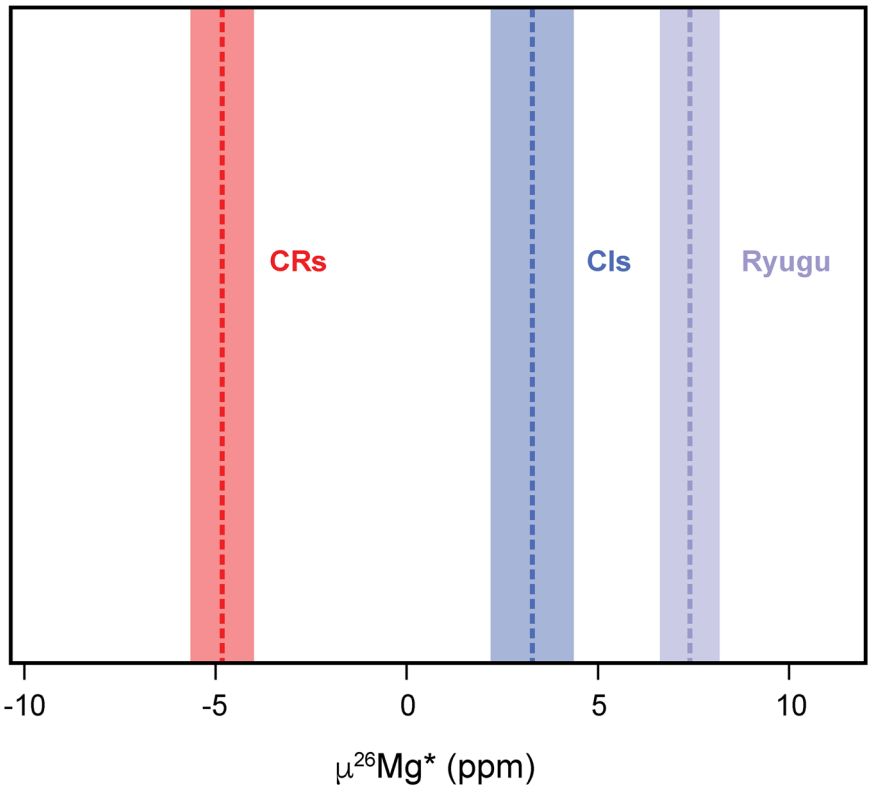

Figure 3. Best estimate of the $\mu^{26}Mg^{*}$ value of Ryugu plotted together with that of the CI and CR parent bodies. Data reflect weighted means with 95% confidence intervals. The CI and CR estimates include data from Larsen et al. (2011), van Kooten et al. (2016), Luu et al. (2019), and van Kooten et al. (2020).

Although our analysis does not allow us to distinguish between ^{26}Al or Mg isotope heterogeneity to account for the range of $\mu^{26}Mg^{*}$ composition across chondrite groups and, in particular, Ryugu's $\mu^{26}Mg^{*}$ excess relative to CIs, future measurements of Ryugu samples may provide insights into this question. Silicon has been recently developed as a novel nucleosynthetic tracer to probe genetic relationships between solar system solids, asteroids, and planetary bodies (Onyett et al. 2023). Carbonaceous chondrites record $\mu^{30}Si$ variability that corresponds to about 23 ppm, with CR and CI chondrite groups defining compositional endmembers. Considering the nucleosynthetic yields of Si and Mg by supernovae, Pringle et al. (2013) suggested that the expected magnitude of heavy-isotope overabundance is larger for Si than for Mg such that any Mg isotope heterogeneity in solar system objects should be accompanied by potentially larger effects for Si. As such, if the $\mu^{26}Mg^{*}$ excess in Ryugu is purely related to nucleosynthetic variability of Mg, then we predict that the $\mu^{30}Si$ value of Ryugu should be markedly more anomalous than CI chondrites. In contrast, identical $\mu^{30}Si$ values between Ryugu and CI would suggest that Ryugu formed from material with a higher initial $^{26}Al/^{27}Al$ relative to the CI chondrite parent body. Clearly, measuring the silicon isotope composition of Ryugu is a timely objective.

4.3. Kinship with the CI Parent Asteroid and the Accretion Region of Ryugu

Several studies have suggested a kinship between Ryugu and CI chondrites based on chemistry, mineralogy, petrology, and nucleosynthetic isotope systematics of various elements (Nakamura et al. 2022, 2023; Hopp et al. 2022; Moynier et al. 2022; Paquet et al. 2023, Yokoyama et al. 2023a). However, some tracers such as ^{54}Cr record variability between Ryugu samples outside of analytical uncertainty, perhaps related to redistribution of presolar carriers during aqueous alteration (Yokoyama et al. 2023b), making the interpretation of these data ambiguous. The high-precision $\mu^{26}Mg^{*}$ data reported here demonstrate, for the first time, a resolvable difference between Ryugu and CI chondrites. Moreover, coupling the $\mu^{26}Mg^{*}$ and $\mu^{25}Mg$ values indicates that unrepresentative sampling must be taken into consideration for some nucleosynthetic tracers, ideally in concert with mass-dependent isotope composition of the same element. Although Ryugu and CI chondrites undoubtedly share many common characteristics, our new Mg isotope data do not support the view that these bodies were sourced from the same precursor material.

It has been proposed that the metal-rich carbonaceous chondrites (CR, CH, and CB chondrites) accreted in the same region as cometary objects based on several lines of evidence, including oxygen isotopes, extreme ^{15}N enrichment, as well as the presence of cometary material in some of these meteorites (Briani et al. 2009; Defouilloy et al. 2017; Nittler et al. 2019). Based on Fe isotopes, Hopp et al. (2022) recently suggested that Ryugu and the parent body of CI chondrites formed beyond the accretion of most carbonaceous chondrite parent bodies. However, CR and CI chondrites (and/or Ryugu) define nucleosynthetic compositional endmembers among carbonaceous chondrite groups in Si, Fe, and Mg (Schiller et al. 2020; Hopp et al. 2022; Onyett et al. 2023). Although this does not preclude that CR, CI, and Ryugu all accreted in the outermost disk, it is difficult to reconcile with the observation that other carbonaceous chondrites record nucleosynthetic compositions

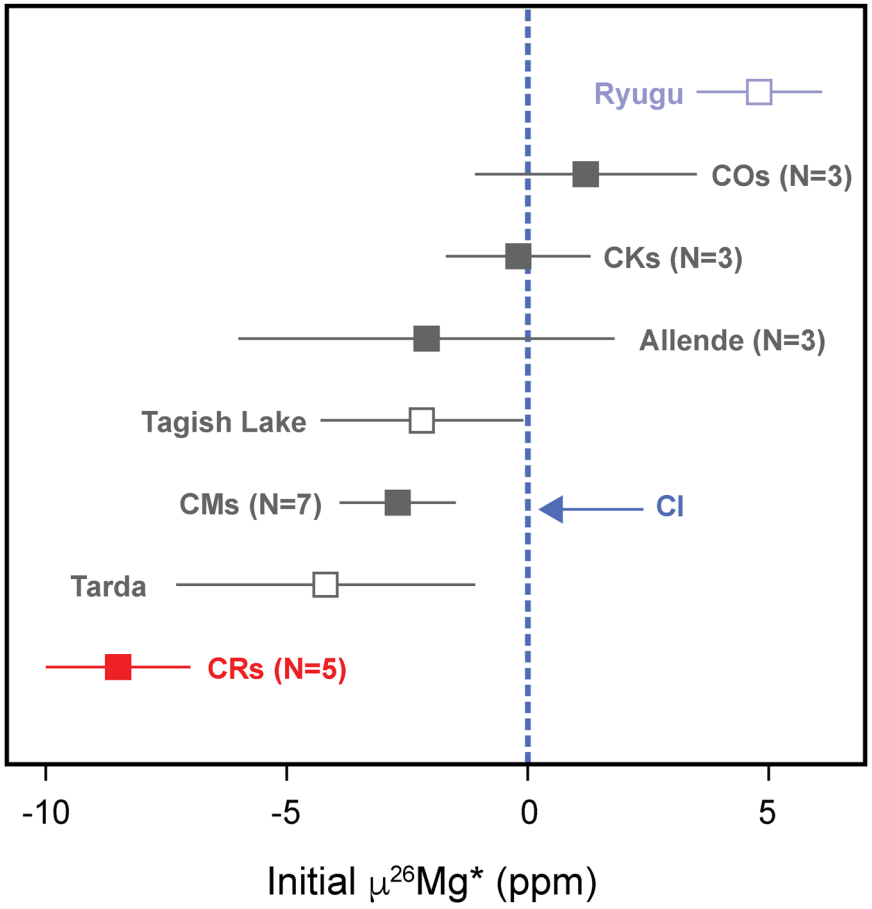

Figure 4. Initial $\mu^{26}Mg^*$ values of Ryugu samples and carbonaceous chondrites plotted relative to the initial $\mu^{26}Mg^*$ value of CI chondrites. All data are weighted means and calculated assuming an initial $^{26}Al/^{27}Al$ ratio of 5.2×10^{-5} (Jacobsen et al. 2008; Larsen et al. 2011) and using the $^{27}Al/^{24}Mg$ of the corresponding reservoirs or individual samples. The initial $\mu^{26}Mg^*$ values of chondrite groups include data from Larsen et al. (2011), van Kooten et al. (2016), Luu et al. (2019), and van Kooten et al. (2020). For CO and CK chondrites as well as Allende, we also included the lower-precision data of Schiller et al. (2010) to calculate the weighted means. Uncertainties are 95% confidence intervals and include the uncertainty of the CI chondrite reservoir.

intermediated between the CR and CI chondrites (and/or Ryugu) endmembers. Evidently, this demonstrates that using nucleosynthetic variations to infer the accretion regions of chondrite parent bodies is complex. Additional high-precision nucleosynthetic isotope data based on larger and representative samples are needed to better understand the relationship between Ryugu and CI chondrites, including their accretion regions. Given the observed Mg isotope variability between Ryugu and CI chondrites, samples returned from Bennu by NASA's OSIRIS-REx mission will be important to explore the extent of nucleosynthetic isotopic diversity across primitive asteroids.

Acknowledgments

This work is carried out under the Hayabusa2 Initial Analysis Team, specifically the Chemistry subteam led by H. Yurimoto. Funding for this project was provided by grants from the Carlsberg Foundation (CF18_1105) and the European Research Council (ERC Advanced grant Agreement 833275—DEEPTIME) to M.B.

ORCID iDs

Martin Bizzarro https://orcid.org/0000-0001-9966-2124
Martin Schiller https://orcid.org/0000-0003-4149-0627
Conel M. O'D. Alexander https://orcid.org/0000-0002-8558-1427
Sachiko Amari https://orcid.org/0000-0003-4899-0974
Audrey Bouvier https://orcid.org/0000-0002-8303-3419
Richard W. Carlson https://orcid.org/0000-0001-7195-2074
Marc Chaussidon https://orcid.org/0000-0001-8475-0690
Wataru Fujiya https://orcid.org/0000-0003-2578-5521
Ryota Fukai https://orcid.org/0000-0002-1477-829X
Ikshu Gautam https://orcid.org/0000-0002-0415-9428
Yuki Hibiya https://orcid.org/0000-0002-3346-9820
Hisashi Homma https://orcid.org/0000-0002-3662-577X
Peter Hoppe https://orcid.org/0000-0003-3681-050X
Tsuyoshi Iizuka https://orcid.org/0000-0001-7896-5812
Akira Ishikawa https://orcid.org/0000-0002-8938-0200
Masanao Abe https://orcid.org/0000-0003-4780-800X

References

Bazi, B., Tack, P., Linder, M., et al. 2022, EP&S, 74, 161
Bizzarro, M., Paton, C., Larsen, K. K., et al. 2011, JAAS, 26, 565
Briani, G., Gounelle, M., Marrocchi, Y., et al. 2009, PNAS, 106, 10522
Carlson, R. W., Boyet, M., & Horan, M. 2007, Sci, 316, 1175
Dauphas, N., & Schauble, E. A. 2016, ArEPS, 44, 709
Defouilloy, C., Nakashima, D., Joswiak, D. J., et al. 2017, E&PSL, 465, 145
Gounelle, M., Schu, F. H., Shang, H., et al. 2001, ApJ, 548, 1051
Greenwood, R. C., Franchi, I. A., Findlay, R., et al. 2023, NatAs, 7, 29
Hopp, T., Dauphas, N., Yoshinari, A., et al. 2022, SciA, 8, eadd8141

Ito, M., Tomioka, N., Uesugi, M., et al. 2022, NatAs, 6, 1163
Jacobsen, B., Yin, Q.-Z., Moynier, F., et al. 2008, E&PSL, 272, 353
Kawasaki, N., Nagashima, K., Sakamoto, N., et al. 2022, SciA, 8, eade2067
Krot, A. N., Nagashima, K., Ciesla, F. J., et al. 2010, ApJ, 713, 1159
Larsen, K. K., Schiller, M., & Bizzarro, M. 2016, GeCoA, 176, 295
Larsen, K. K., Trinquier, A., Paton, C., et al. 2011, ApJL, 735, L37
Larsen, K. K., Wielandt, D., Schiller, M., Krot, A. N., & Bizzarro, M. 2020, E&PSL, 535, 116088
Lee, T., Papanastassiou, D. A., & Wasserburg, G. J. 1976, GeoRL, 3, 41
Luu, T.-H., Hin, R. H., Coath, C. D., & Elliott, T. 2019, E&PSL, 522, 166
Moynier, F., Dai, W., Yokoyama, T., et al. 2022, GChP, 24, 1
Nakamura, E., Kobayashi, K., Tanaka, R., et al. 2022, PJAB, 98, 227
Nakamura, T., Matsumoto, M., Amano, K., et al. 2023, Sci, 6634, abn8671
Nittler, L. R., Stroud, R. M., Trigo-Rodríguez, J. M., et al. 2019, NatAs, 3, 659
Okazaki, R., Marty, B., Busemann, H., et al. 2023, Sci, 379, abo0431
Olsen, M. A., Wielandt, D., Schiller, M., et al. 2016, GeCoA, 191, 118
Onyett, I. J., Schiller, M., & Makhatadze, G. 2023, Nat, 619, 539
Palme, H., Lodders, K., & Jones, A. 2014, in Planets, Asteroids, Comets and The Solar System, Treatise on Geochemistry, ed. A. M. Davis, Vol. 2 (2nd ed.; Amsterdam: Elsevier), 15
Paquet, M., Moynier, F., Yokoyama, T., et al. 2023, NatAs, 7, 182
Park, C., Nagashima, K., Krot, A. N., et al. 2017, GeCoA, 201, 6
Paton, C., Schiller, M., Ulfbeck, D., & Bizzarro, M. 2012, JAAS, 27, 644
Pringle, E. A., Savage, P. S., & Jackson, M. 2013, ApJ, 779, 123
Schauble, E. A. 2011, GeCoA, 75, 844
Schiller, M., Handler, M., & Baker, J. A. 2010, E&PSL, 297, 165
Schiller, M., Paton, C., & Bizzarro, M. 2015, GeCoA, 149, 88
Schiller, M., Siebert, J., & Bizzarro, M. 2020, SciA, 6, eaay7604
Tachibana, S., Sawada, H., Okazaki, R., et al. 2022, Sci, 375, 101
Torrano, Z. A., Jordan, M. K., Mock, T. D., et al. 2023, LPI Contribution, 2806, 1776
Trinquier, A., Birck, J.-L., & Allègre, C. J. 2007, ApJ, 655, 1179
Trinquier, A., Elliott, T., Ulfbeck, D., Krot, A. N., & Bizzarro, M. 2009, Sci, 324, 374
van Kooten, E., Calvalcante, L., Wielandt, D., & Bizzarro, M. 2020, M&PS, 55, 575
van Kooten, E., Wielandt, D., Schiller, M., et al. 2016, PNAS, 113, 2011
Walkiewicz, T. A., Raman, S., Jurney, E. T., Starner, J. W., & Lynn, J. E. 1992, PhRvC, 45, 1597
Wasserburg, G. J., Wimpenny, J., & Yin, Q.-Z. 2012, M&PS, 47, 1980
Watanabe, S., Hirabayashi, M., Hirata, N., et al. 2019, Sci, 364, 268
Yamaguchi, A., Tomioka, N., Ito, M., et al. 2023, NatAs, 7, 398
Yokoyama, T., Nagashima, K., Nakai, I., et al. 2023a, Sci, 379, 7850
Yokoyama, T., Wadhwa, M., Iizuka, T., et al. 2023b, SciA, 9, eadi7048
Yoshimura, T., Araoka, D., Naraoka, H., et al. 2023, Nat. Commun, submitted
Young, E. D., & Galy, A. 2004, RvMG, 55, 197